

Experimental study of a micro combined heat and power system: characterization of the parabolic trough collector used for direct steam generation

Jean-Louis Bouvier^{1,2}, Ghislain Michaux¹, Patrick Salagnac¹, François Nepveu³, Dominique Rochier³, Thiebaut Kientz²

¹ LaSIE, Université de La Rochelle, La Rochelle (France)

² Exoès, Gradignan (France)

³ Exosun, 33650 Martillac, (France)

Summary

An experimental campaign has been conducted on a solar parabolic trough collector used in a micro CHP system for direct steam generation. The study of the solar field only, and its thermal characterization, which are reported here, are the first step of the global characterization of the CHP system. Main particularities of the solar field are the two axis tracker and its relatively small size (46.5 m² of solar aperture area). It is tested under direct steam generation with demineralized water. At first, performances of the collector during two typical days, namely a sunny day and a cloudy day, are presented. On the sunny day, the system produced, during 7 hours, saturated steam with a quality (mass fraction of vapor) higher than 0.5 for a flow rate of 30 kg.h⁻¹. Then, a study of the thermal efficiency based on on-sun steady state tests is conducted for different working and meteorological conditions. The obtained value of the heat losses coefficient is compared to off-sun measurements. The reached thermal efficiency (around 50%) leads to performances that are suitable for the coupling with the steam engine.

Keywords: Solar thermal energy, parabolic trough collector, experimentation, direct steam generation.

Nomenclature

A: aperture area [m²]

a₁: heat losses coefficient [W.m⁻².K⁻¹]

a₂: temperature dependence of the heat losses [W.m⁻².K⁻²]

G_b: direct normal solar irradiance [W.m⁻²]

h: enthalpy [J.kg⁻¹]

\dot{m} : flow rate [kg.s⁻¹]

p: pressure [bar]

T: temperature [°C]

T_m^{*}: reduced temperature difference [K.m².W⁻¹]

Greek symbols

η: efficiency [-]

φ: heat flux [W]

Subscripts

0: optical

c: collector

ext: ambient

f: fluid

m: mean

s: solar

1. Introduction

Due to the depletion of fossil fuels and to the increase in electrical energy consumption in buildings, it becomes necessary to develop new solutions that respond to these new needs. Micro Combined Heat and Power (CHP) are one of the recent solutions working with renewable energy sources that can be integrated in future positive energy buildings.

In the frame of the development project of a micro solar CHP, a solar concentrator (parabolic trough) has been coupled to a Hirn (or superheated Rankine) cycle engine. The concentrator brings the thermal energy required by the engine at an important level of temperature and pressure. It has been dimensioned for a low output power (around 20 kW) in order to fulfil the energy requirements of residential or commercial buildings, but with a high output temperature (around 250°C) to be able to produce steam.

The simplified diagram of the cycle is shown in Figure 1. Demineralized water enters the solar collectors at a pressure between 10 and 30 bars with a flow rate between 20 and 40 kg.h⁻¹. Steam is generated in the absorber tube at a temperature from 180°C to 250°C. This steam is admitted in the reciprocating engine and then condensed. Heat, recovered by the hydraulic system, is finally dissipated in a cooling loop used to simulate a building consumption.

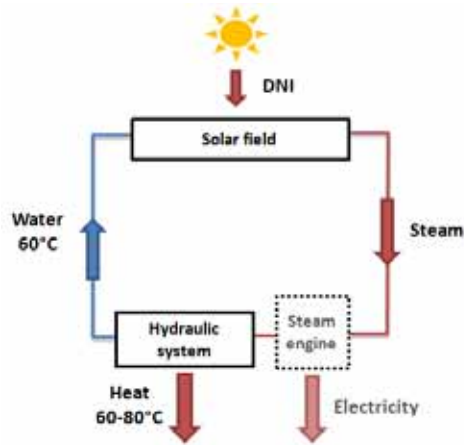


Figure 1: Schematic diagram of the micro CHP system.

Main particularities of this system are the two axis tracker and its relative small size (46.5 m² of solar aperture area). It has been assembled by the company Exosun at La Rochelle (France).

Direct steam generation has been widely studied in the case of large solar fields (Eck et al., 2003; Fernández-García et al., 2010; Hirsch et al., 2014; Krüger et al., 2012; Montes et al., 2011). In comparison to large size systems, the flow rate required to generate steam in the case of smallest systems is lower. This low flow rate leads to a significant difference in dynamic behavior. For small scale systems with steam generation, Almanza *et al.* (1997) generated saturated steam at a temperature of 130°C with a parabolic trough collector of 36,3 m², Kalogirou *et al.* (1997) performed experiments using a flash system with a collector surface of 3.5 m². The study of the solar field only, is the first step of the global characterization of the system. For this reason, the engine has been removed during tests. The performances of the system on a typical sunny day and a cloudy day are presented. Then, a steady state study of the efficiency is carried out.

2. Experimental set-up

The experimental prototype is composed of four main elements: a structure equipped with a solar parabolic trough collector, an electrical superheater, a hydraulic system, and a cooling loop.



Figure 2: Outside view of the micro CHP system.

The collector is composed by a linear parabolic-shaped reflector and a solar receiver which consists of an absorber tube protected by a glass envelope. The space between the glass and absorber tubes is at atmospheric pressure (non-evacuated tube). The absorber is a stainless tube with a selective coating. The reflectors are built with a film of anodized aluminum bonded to a composite material. The collector is located on a structure that allows a two axis tracking (Figure 2). The advantage of two axis tracker is that the collector always receives maximum available radiation (incidence angle is always zero). The aperture length of 1.94 m leads to a total aperture area of 46.5 m² with a concentration ratio (aperture area over absorber area) of 18.1 (CEN, 2000). Optical properties of the collector are given in table 1.

Table 1: Optical properties of the collector

Absorber absorptance (solar radiation)	0.95
Absorber emittance (100°C)	0.15
Mirror reflectance	0.81

A superheater of 5 kW (Figure 3) has been added at the end of the absorber in order to ensure that the exiting fluid is superheated steam. Unlike saturated steam, it is possible, with superheated steam, to determine its enthalpy knowing the temperature and pressure values. The cooling loop can supply cold water with a typical flow rate of 800 kg.h⁻¹ and a temperature ranging from 35°C to 70°C.

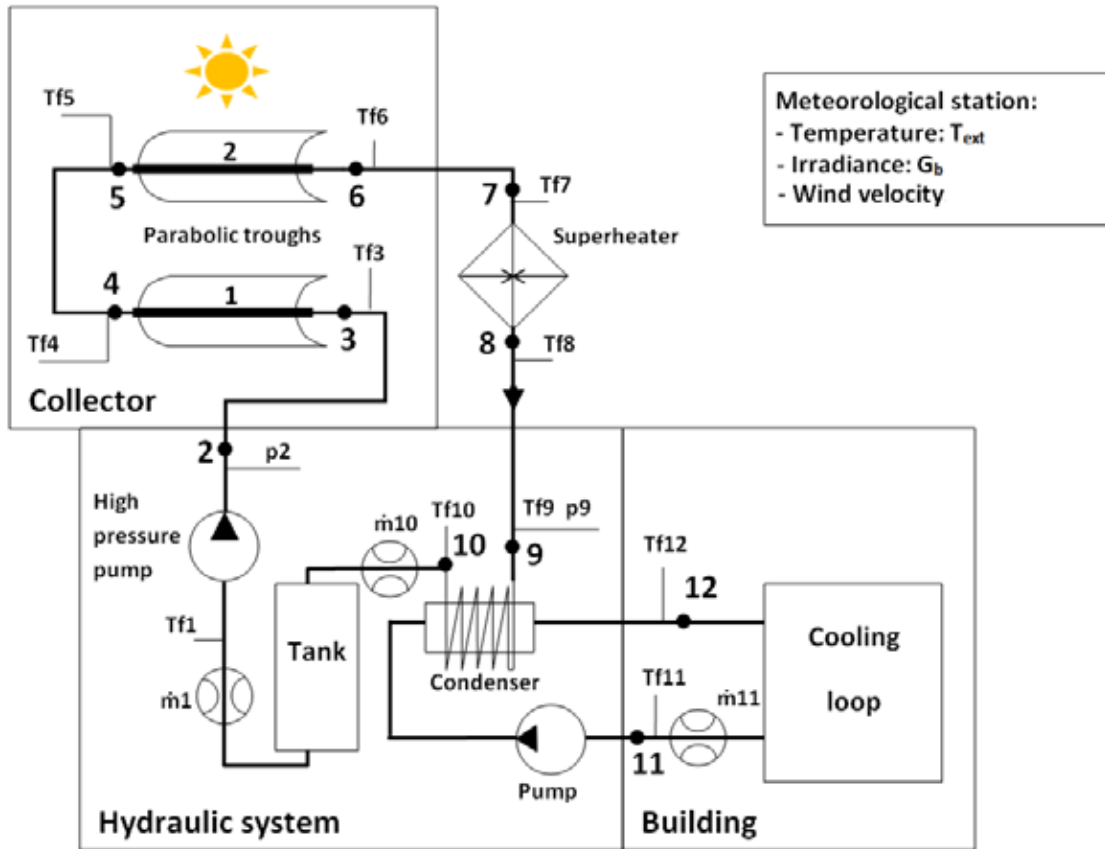


Figure 3: Schematic diagram of the studied system.

This experimental setup allows the monitoring of the meteorological conditions and of the fluid temperature, pressure and flow rate at several locations (Figure 3). DNI is measured by a pyrheliometer which is positioned on the concentrator itself. Thus, the measured value exactly corresponds to the one received by the mirrors. Temperature sensors (thermocouples type K) are installed at the inlet and outlet of each line of absorber and of the superheater (Tf_3 , Tf_4 , Tf_5 , Tf_6 , Tf_7 and Tf_8). RTD are used to measure the temperature at the inlet and outlet of the cooling loop (Tf_{11} , Tf_{12}). The volumetric flow rate in the cooling loop (\dot{m}_{11}) is measured by a vortex flow sensor. Volumetric flow rates at the inlet and outlet of the solar loop (\dot{m}_1 and \dot{m}_{10}) are evaluated by turbine flow sensors. Pressure sensors are located at the inlet and outlet of the hydraulic system (p_2 and p_9). Electrical consumptions of the cooling loop, superheater as well as tracking and hydraulic systems are measured by energy meters. RTD and turbine flow sensors have been calibrated. The uncertainties given in Table 2 are calculated according to the GUM (BIPM et al., 2008). All the uncertainties appearing in the graphs are calculated with a coverage factor of 2, corresponding to a confidence level of 95 %.

Table 2: Uncertainties of the sensors.

Sensors	Standard uncertainty
Tf_1 , Tf_{11} , Tf_{12}	0.19°C
Tf_3 , Tf_4 , Tf_5 , Tf_6 , Tf_7 , Tf_8 ($T < 375^\circ\text{C}$)	1.9°C
Tf_9 , Tf_{10} ($T < 333^\circ\text{C}$)	2.1°C
\dot{m}_{10} , \dot{m}_9	0.36 kg.h ⁻¹
\dot{m}_{11}	0.6 kg.min ⁻¹
p_2 , p_9	0.36 bar

Direct Normal Irradiance - G_b	1.2 %
Ambient temperature - T_{ext}	0.12°C
Electrical power	0.6 - 0.9 %

3. Experimental evaluation of the thermal efficiency

From experimental results, the efficiency is evaluated using the definition:

$$\eta_c = \frac{\phi_c}{\phi_s} \quad (\text{Eq. 1})$$

where ϕ_s , the solar power input, is calculated from the DNI G_b , and the aperture area A as follows:

$$\phi_s = A G_b \quad (\text{Eq. 2})$$

The output thermal power of the collector, ϕ_c , can be expressed as follows:

$$\phi_c = \dot{m}_{10} h_6 - \dot{m}_1 h_3 \quad (\text{Eq. 3})$$

And in the case of steady state flow regime by:

$$\phi_c = \dot{m}_1 (h_6 - h_3) = \dot{m}_{10} (h_6 - h_3) \quad (\text{Eq. 4})$$

where h_6 can be calculated from the enthalpy h_9 or from an energy balance on the condenser. Note that the enthalpies subscripts refer to the point numbers in Figure 3.

4. Results

4.1. Typical sunny and cloudy days

Results obtained for typical sunny and cloudy days are presented in Figure 4. It can be noticed that, since values are not relevant for unbalanced states, evolutions of the instantaneous efficiency and output steam quality are not plotted for the cloudy day. It can be observed in Figure 4 (left) that the instantaneous efficiency being almost constant between 9:30 and 19:20, the power and the steam quality nearly follow the irradiance. A small disturbance is observed around noon. It is certainly due to an absorber positioning issue. This issue has been corrected for the efficiency tests presented hereafter. In the Figure 4 (right), both the solar and output powers show sharp variations. They are explained by output flow rate discrepancies due to the stop of vaporization process when the irradiance ceases. However, the inertia of the system allows the output power to stay in a limited range of variation if the cut in irradiance is not too long as it can be seen from 15:30 to 16:30 in Figure 4 (right).

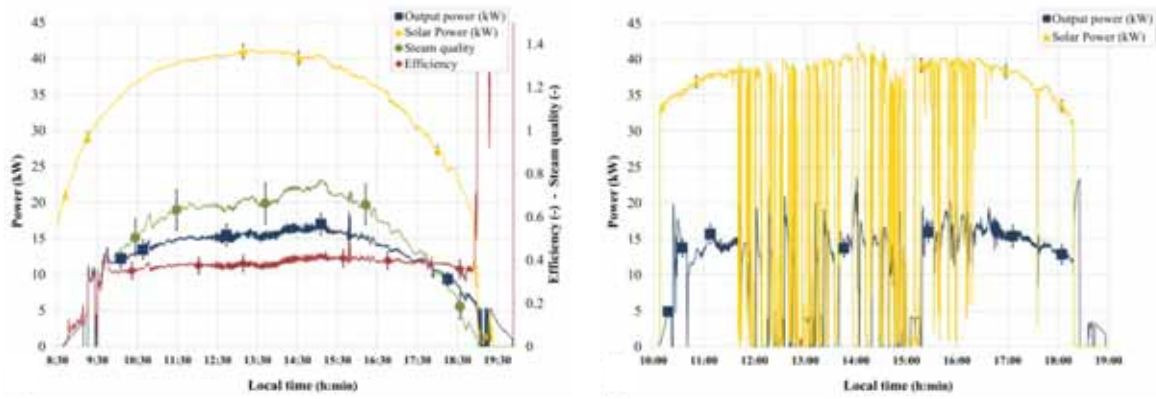


Figure 4: Power, instantaneous efficiency and outlet steam quality evolutions on a sunny day (left) and power evolutions on a cloudy day (right).

4.2. Efficiency

The steady state efficiency is commonly defined as (CEN, 2001) (Perers, 1997) (Fischer et al., 2006) (Janotte et al., 2009):

$$\eta_c = \eta_0 - a_1 T_m^* - a_2 G (T_m^*)^2 \quad (\text{Eq. 5})$$

where η_0 is the optical efficiency, a_1 the heat losses coefficient and a_2 the temperature dependence of the heat losses coefficient.

The reduced temperature difference T_m^* is defined as follows:

$$T_m^* = \frac{T_m - T_{ext}}{G} \quad (\text{Eq. 6})$$

where T_m is the average temperature of the fluid:

$$T_m = \frac{Tf_0 + Tf_3}{2} \quad (\text{Eq. 7})$$

Steady state tests have been performed with a flow rate of $30 \text{ kg}\cdot\text{h}^{-1} \pm 10\%$, irradiance between 728 and $889 \text{ W}\cdot\text{m}^{-2}$ and outside temperature between 17.1 and 19.2°C . The obtained thermal efficiency values are plotted in Figure 5.

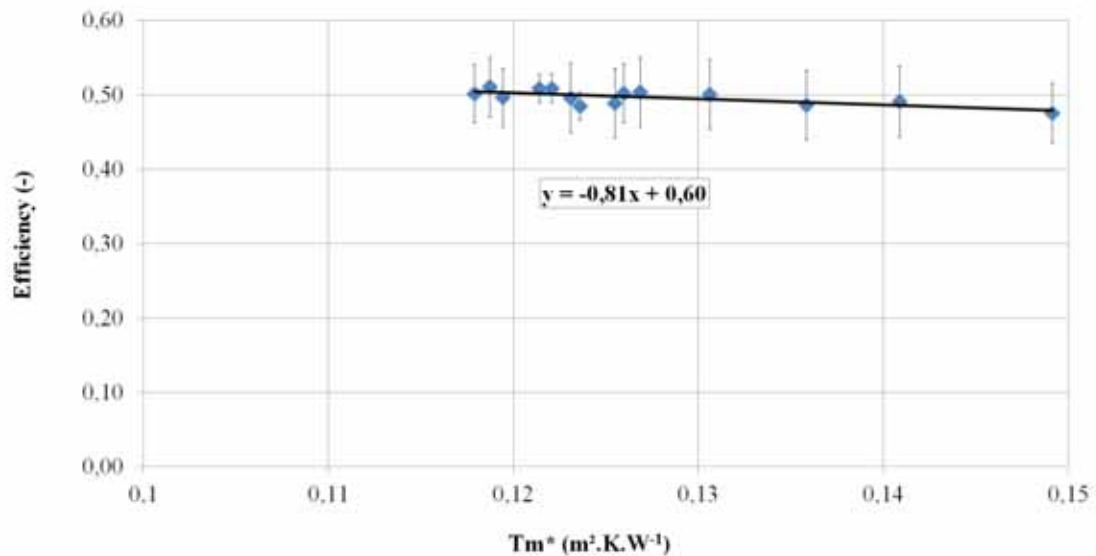


Figure 5: Thermal efficiency as a function of T_m^* .

The limited range of values of T_m^* obtained during the experiment explained the low variation of the efficiency. In conventional systems with a relatively high flow rate, the difference between inlet and outlet temperature during tests is low, the average fluid temperature and thus the T_m^* are strongly dependent of the inlet temperature. A large range of T_m^* ratios can be tested by varying the inlet temperature (Janotte et al., 2009). In small size systems with direct steam generation, the average fluid temperature (T_m) is always elevated. In order to be relevant the tests should be performed within a limited range of inlet flow rate and irradiance (CEN, 2001). These limitations do not allow a large variation of the T_m^* ratio.

The reached efficiency is consistent with values observed in the literature for small scale systems with steam generation: 42 % ($T_m^* \approx 0.06 \text{ K.m}^2.\text{W}^{-1}$ (Almanza et al., 1997)) and 48.9 % ($T_m^* \approx 0.14 \text{ K.m}^2.\text{W}^{-1}$ (Kalogirou et al., 1997)). The optical efficiency is around 60 %. This value is relevant regarding the measured mirrors reflectance of 81 %. With a first order estimation (a_2 neglected), the reached value for a_1 is $0.81 \text{ W.K}^{-1}.\text{m}^{-2}$ (Eq. 5). Off-sun measurements have been performed to determine the heat losses coefficient and give a result for a_1 of $0.42 \text{ W.K}^{-1}.\text{m}^{-2}$. The difference between on-sun and off-sun results is due to the fact that both the glass envelope and the absorber tube temperatures are higher when they are heated by the sun (Eck et al., 2010).

5. Conclusion

A characterization of a unique prototype of parabolic trough collector, with direct steam generation and a two axis tracking system, has been performed. The correct operation of the system for sunny and cloudy days has been verified. The efficiency of the concentrator could be defined following the classical T_m^* approach with on-sun and off-sun tests. The next step of the project is now the experimental characterization of the complete micro-CHP system including the steam engine.

6. References

- Almanza, R., Lentz, A., Jiménez, G., 1997. Receiver behavior in direct steam generation with parabolic troughs. *Solar Energy* 61, 275–278.
- BIPM, I., IFCC, I., ISO, I., 2008. Evaluation of measurement data-Guide to the expression of uncertainty in measurement.
- CEN, 2000. European standard EN ISO 9488:2000, Solar energy - Vocabulary.
- CEN, 2001. European standard EN12975-2:2001, Solar thermal systems and components-Solar collectors – Part 2.
- Eck, M., Feldhoff, J.F., Uhlig, R., 2010. Thermal modelling and simulation of parabolic trough receiver tubes, in: *Proceedings of the ASME 2010 4th International Conference on Energy Sustainability*. pp. 659–666.
- Eck, M., Zarza, E., Eickhoff, M., Rheinländer, J., Valenzuela, L., 2003. Applied research concerning the direct steam generation in parabolic troughs. *Solar Energy* 74, 341–351.
- Fernández-García, A., Zarza, E., Valenzuela, L., Pérez, M., 2010. Parabolic-trough solar collectors and their applications. *Renewable and Sustainable Energy Reviews* 14, 1695–1721. doi:10.1016/j.rser.2010.03.012
- Fischer, S., Lüpfert, E., Müller-Steinhagen, H., 2006. Efficiency testing of parabolic trough collectors using the quasi-dynamic test procedure according to the European Standard EN 12975, in: *Proceedings of the 13th SolarPACES Conference. Concentrating Solar Power and Chemical Energy Technologies*, Seville, Spain.
- Hirsch, T., Feldhoff, J.F., Hennecke, K., Pitz-Paal, R., 2014. Advancements in the Field of Direct Steam Generation in Linear Solar Concentrators—A Review. *Heat Transfer Engineering* 35, 258–271. doi:10.1080/01457632.2013.825172
- Janotte, N., Meiser, S., Krüger, D., Lüpfert, E., Pitz-Paal, R., Fischer, S., Müller-Steinhagen, H., 2009. Quasi-dynamic analysis of thermal performance of parabolic trough collectors, in: *Proceedings of the 15th SolarPACES Conference*. Berlin, Germany.

Kalogirou, S., Lloyd, S., Ward, J., 1997. Modelling, optimisation and performance evaluation of a parabolic trough solar collector steam generation system. *Solar Energy* 60, 49–59.

Krüger, D., Krüger, J., Pandian, Y., O’Connell, B., Feldhoff, J.F., Karthikeyan, R., Hempel, S., Muniasamy, K., Hirsch, T., Eickhoff, M., Hennecke, K., 2012. Experiences with Direct Steam Generation at the Kanchanaburi Solar Thermal Power Plant, in: *Proceedings of the 18th SolarPACES Conference*. Marrakech, Morocco.

Montes, M.J., Rovira, A., Muñoz, M., Martínez-Val, J.M., 2011. Performance analysis of an Integrated Solar Combined Cycle using Direct Steam Generation in parabolic trough collectors. *Applied Energy* 88, 3228–3238. doi:10.1016/j.apenergy.2011.03.038

Perers, B., 1997. An improved dynamic solar collector test method for determination of non-linear optical and thermal characteristics with multiple regression. *Solar Energy* 59, 163–178.

7. Acknowledgements

The authors want to thank the Poitou-Charentes Regional Council and the European Union (FEDER) for their financial contributions as well as the Exosun and Exoès companies in charge respectively of the structure and of the parabolic trough collector and, of the hydraulic system and steam engine.